energies

MDPI

Article

Energy and Environmental Impacts of Replacing Gasoline with LPG Under Real Driving Conditions

Edward Kozłowski [1,*], Alfredas Rimkus [2], Magdalena Zimakowska-Laskowska [3], Jonas Matijošius [4], Piotr Wiśniowski [3], Mateusz Traczyński [1], Piotr Laskowski [5] and Radovan Madlenak [6]

[1] Faculty of Management, Lublin University of Technology, 38D Nadbystrzycka Str., 20-618 Lublin, Poland; m.traczynski@pollub.pl
[2] Department of Automobile Engineering, Faculty of Transport Engineering, Vilnius Gediminas Technical University-VILNIUS TECH, Plytinės Str. 25, LT-10105 Vilnius, Lithuania; alfredas.rimkus@vilniustech.lt
[3] Environment Protection Centre, Motor Transport Institute, 80 Jagiellońska Str., 03-301 Warsaw, Poland; magdalena.zimakowska-laskowska@its.waw.pl (M.Z.-L.); piotr.wisniowski@its.waw.pl (P.W.)
[4] Mechanical Science Institute, Vilnius Gediminas Technical University-VILNIUS TECH, 25 Plytinės Str., LT-10105 Vilnius, Lithuania; jonas.matijosius@vilniustech.lt
[5] Faculty of Automotive and Construction Machinery Engineering, Warsaw University of Technology, 84 Narbutta Str., 02-524 Warsaw, Poland; piotr.laskowski@pw.edu.pl
[6] Faculty of Operation and Economics of Transport and Communications, University of Žilina, Univerzitna 8215/1, 010 26 Žilina, Slovakia; radovan.madlenak@uniza.sk
* Correspondence: e.kozlovski@pollub.pl

Abstract

This study investigates the energy and environmental implications of replacing E10 gasoline with Liquefied Petroleum Gas (LPG) in a Euro 4 passenger car under real-world urban driving conditions. A comparative methodology robust to operating-state distribution was applied, combining portable exhaust gas analysis with on-board diagnostic data to calculate energy-specific emissions per crankshaft revolution and to reconstruct emission surfaces in the load–RPM domain using bilinear interpolation. The study revealed that LPG reduces carbon dioxide emissions by 8.35%, demonstrating a clear climate and energy benefit due to its lower carbon intensity. In comparison, carbon monoxide (+9.5%) and hydrocarbons (+8.3%) increased under low-load and idle conditions. Nitrogen oxides showed only minor differences between the fuels (+1.3%). LPG exhibited a more stable CO_2 emission profile, reflecting improved combustion efficiency from an energy perspective, although its performance in terms of incomplete combustion products requires further optimisation. The methodology highlights how linking energy efficiency with pollutant formation provides a comprehensive framework for evaluating alternative fuels in Real Driving Emissions (RDE) tests. The results confirm LPG's potential to reduce greenhouse gas emissions in transport systems and identify calibration strategies needed to mitigate trade-offs in local pollutant emissions.

Keywords: fuel; energy efficiency; specific emission

check for updates

Academic Editor: Roberto Finesso

Received: 16 September 2025
Revised: 14 October 2025
Accepted: 17 October 2025
Published: 20 October 2025

Citation: Kozłowski, E.; Rimkus, A.; Zimakowska-Laskowska, M.; Matijošius, J.; Wiśniowski, P.; Traczyński, M.; Laskowski, P.; Madlenak, R. Energy and Environmental Impacts of Replacing Gasoline with LPG Under Real Driving Conditions. *Energies* **2025**, *18*, 5522. https://doi.org/10.3390/en18205522

Copyright: © 2025 by the authors. Licensee MDPI, Basel, Switzerland. This article is an open access article distributed under the terms and conditions of the Creative Commons Attribution (CC BY) license (https://creativecommons.org/licenses/by/4.0/).

1. Introduction

Road transport remains a major source of urban air pollution and greenhouse gas emissions, notably carbon monoxide (CO), hydrocarbons (HC), nitrogen oxides (NOx), particulate matter (PM/PN), and carbon dioxide (CO_2). Liquefied petroleum gas (LPG), due to its lower carbon content and distinct combustion characteristics, can reduce both the carbon footprint and exhaust pollutants compared to gasoline. With the increasing use

of portable measurement systems, real driving emissions (RDE) testing now captures the dynamic effects of engine load and speed on instantaneous emissions [1–3]. However, even on identical routes, engine operating conditions often differ between fuels due to driving style, traffic density, and vehicle dynamics, making conventional distance-based indicators (g/km) potentially misleading.

This study introduces a methodology that enables fuels to be compared through the lens of engine operation, rather than mileage, by utilising specific emissions per crankshaft revolution and interpolation within the load–RPM space. By integrating instantaneous emission analysis with probability density distributions of operating states, the method provides a more robust and comparable assessment of pollutant formation under real-world conditions.

We apply this approach to compare CO_2, CO, NOx, and HC emissions of an E10- and LPG-fuelled vehicle during urban driving. The proposed methodology enables an objective evaluation of both fuels by linking combustion efficiency with emission variability, revealing how operational factors shape the environmental performance of alternative fuels.

Novelty of the research:

1. When a vehicle is driven under real-world conditions (not following a set cycle) [4], it is not possible to compare emissions when the vehicle is powered by different fuels. On the one hand, the distance travelled is the same, but on the other hand, due to real-world conditions when driving in urban areas, the time spent waiting at intersections/traffic lights varies. On the other hand, due to driving technique, the dynamics of the vehicle in real conditions, and thus the characteristics of the engine performance, must be taken into account.
2. In real conditions, the time taken to cover the same distance varies.
3. Engine load has a significant impact on emissions. Therefore, in order to compare the pollutants generated by an internal combustion engine in real conditions, the unit emissions (emissions per crankshaft revolution) were compared, taking into account the engine load during driving.

The study compared CO_2, CO, NOx and HC emissions during passenger car travel in real conditions and powered by different fuels.

In order to compare pollutant emissions, engine load [kW], engine speed (revolutions per minute) and pollutant volume were analysed [g/kWh]. Let $\left\{\left(L_i^c, R_i^c, x_i^c\right)\right\}_{0\leq i\leq n^c}$ be a sequence of readings during the journey, where L_i^c denotes the engine load [kW] when the engine was powered by fuel $c \in \{E10, LPG\}$, R_i^c is revolutions per minute, and x_i^c is emissions [g/kWh] at $i-$th moment, $0 \leq i \leq n^c$. Figure 2 illustrates that the number of readings during the tests when the vehicle was powered by different types of fuel varies (i.e., $n^{E10} \neq n^{LPG}$).

In many cases, we use stochastic processes to describe the behaviour of technical systems/vehicles, e.g., semi-Markov models [5–7]. To identify dependencies in technical systems [8–12], we can use various machine learning methods [13,14].

When analysing the pollution generated by combustion engines, it is also necessary to identify the driving style, which directly affects the level of pollution [15], as well as the conditions in which the vehicle is used [16]. In these cases, we analyse the impact of vehicle driving dynamics, namely speed and acceleration, on the amount of pollution. Vehicle dynamics directly depend on engine operating parameters.

However, the question arises how engine performance characteristics (engine operation) directly affect the amount of pollution. By analysing engine performance, we can not only compare pollution caused by vehicles, but also pollution generated by sta-

tionary combustion engines, engines installed on boats, rail vehicles, and all types of combustion engines.

2. Literature Review

Real-world emission studies clearly show that LPG-powered vehicles systematically emit less CO_2 and CO than gasoline-powered cars, with CO_2 reductions typically in the range of 5–20% and CO emission reductions reaching up to several dozen per cent, depending on the type of engine, calibration, and test conditions [1–3,17–19]. At the same time, the differences in NOx and HC are less clear, with some studies pointing to the advantage of gasoline. In contrast, others emphasise comparable emission levels, depending on the vehicle's engine design and technical condition. LPG's advantage in reducing particulate matter count and mass is particularly pronounced, especially in newer vehicle generations, where PN/PM reductions of up to 90% compared to gasoline are observed [20–22]. However, these benefits are limited in older or poorly maintained vehicles [22,23]. The most consistent effects of LPG are seen in CO emissions. Numerous meta-analyses and experimental studies confirm a reduction in this pollutant from approximately 11% to over 60%, which is explained by more homogeneous fuel mixing in the gas phase and a simpler chemical composition [17,24–26]. The differences are particularly noticeable in urban conditions and at idle speeds, where LPG significantly reduces CO emissions [27]. However, the results regarding NOx are much less clear. Some authors report a slight increase in HC emissions when fuelled with LPG, due to higher combustion temperatures and earlier ignition [17], while other studies indicate significant reductions, up to 41% in four-stroke engines and 64% in two-stroke engines [24,28]. These differences are mainly due to different combustion strategies, excess air ratios, ignition settings, and engine design parameters [29].

Regarding HC emissions, modern LPG-powered vehicles with efficient exhaust gas aftertreatment systems typically generate lower values than gasoline-powered cars [3,28,30]. However, in older units, or in cases of poor system calibration, these emissions may be comparable or even higher [22,31]. The qualitative composition of hydrocarbons is also important. LPG emits more light alkanes, while gasoline produces more aromatics and olefins with a higher ozone formation potential, which makes LPG more beneficial in terms of secondary photochemical smog [32]. In conditions common in urban traffic, such as stops at traffic lights or light driving, LPG offers a particularly significant advantage, reducing CO and HC emissions by up to 60% and reducing particulate matter by approximately 70%, while also leading to a 10–18% reduction in CO_2 emissions [2,3,17,20,27]. The only exception is nitrogen oxides, whose emissions may be slightly higher under these conditions. With respect to CO_2, studies consistently confirm the superior performance of LPG, with reductions ranging from 1.7% to 15% compared to gasoline in both laboratory and on-road conditions [2,3,33]. From a life-cycle perspective, total greenhouse gas emissions for LPG are approximately 10–20% lower [34,35], and even greater reduction potential is associated with bio-LPG, which reduces the carbon footprint by up to 80% compared to conventional fuels [36]. Regardless of the fuel type, engine load and speed have a key impact on emissions. An increase in load typically leads to increased CO_2, NOx, and, to some extent, CO and HC emissions, especially at low vehicle speeds [37,38]. However, the relationship between emissions and engine speed can be nonlinear, with NOx increasing up to a certain threshold and decreasing due to a shorter residence time in the cylinder [21,39]. This means that reliable comparisons of fuels require analysis of engine operating schedules and consideration of the frequency of individual states.

Traditionally, emissions are reported per unit of distance (g/km), which complies with regulations but averages out variable operating conditions and fails to capture short-term

emission peaks. Analysing instantaneous emissions based on load and engine speed allows for a more accurate assessment of combustion dynamics and the relationship between operating state and emissions, but requires a more sophisticated analytical approach [40,41]. It is increasingly emphasised that both methods should be combined to provide a complete picture of emissions characteristics [42]. The literature also highlights the existence of emission trade-offs: reducing CO_2, CO, and HC is often associated with a slight increase in NOx, which is particularly true for alternative fuels [43,44]. In the case of LPG, the advantages in greenhouse gas and particulate matter emissions may be offset by higher NOx values under certain operating conditions, especially at high loads and engine speeds [3,17].

In summary, current research results indicate that LPG is a fuel with significant environmental potential. However, traditional emissions comparisons in g/km units do not clarify the extent to which the observed differences are due to fuel characteristics alone and to what extent to different engine operating patterns. Therefore, an approach that considers load and engine speed distributions and analyses emissions in relation to a unit of engine operation, for example, specific emissions per crankshaft revolution, is necessary. This methodology, combining bilinear interpolation with probability density analysis of engine operating states, is used in the remainder of this article, allowing for an objective comparison of the emission characteristics of gasoline and LPG in real-world urban traffic.

3. Experimental Setup and Methodology

3.1. Experimental Research of Real Driving in Urban Conditions

Urban real driving emissions tests were conducted using a Subaru Outback III AWD with a gasoline engine (EJ253). The gasoline was supplied via a multi-point fuel injection system. The engine's maximum power output is 127 kW, with a peak torque of 229 Nm, and it complies with the EURO 4 emission standard. The vehicle was additionally fitted with an OSCAR-N LPG fuel supply system. During testing, the engine operated on commercial E10 gasoline (90% gasoline + 10% bioethanol) or liquefied petroleum gas (LPG).

The real driving in urban conditions route was established on public roads in Vilnius, encompassing streets with varying traffic intensities and traffic control measures such as traffic lights, roundabouts, and speed bumps (Figure 1). The road profile was not level, including both ascents and descents. In certain sections of the route, traffic conditions were dense, with a maximum permissible speed of 50 km/h, while other sections passed through lower-traffic areas with higher speed limits of up to 70 km/h. The route was completed over a total distance of 10.4 km within approximately 14 min, starting and ending at the same location.

Depending on the traffic conditions and the type of fuel used, the engine operated at different speeds; however, the difference in vehicle driving time was insignificant (Figure 2).

Figure 2 shows the engine speed (RPM) versus time curve during real-world driving. The variation in performance characteristics is visible depending on the fuel used: for E10 gasoline (red line) and LPG (blue, dashed line). The differences in the curves reflect different load profiles and engine dynamics during the drive.

Pollutant emissions were comprehensively determined using a portable gas analyser and vehicle diagnostic equipment. The MRU "Nova Plus" portable gas analyser was installed in the vehicle, with the gas sampling probe mounted in the exhaust pipe downstream of the catalytic converter. Exhaust gas composition data were recorded every 1 s. The main technical specifications of the analyser are presented in Table 1.

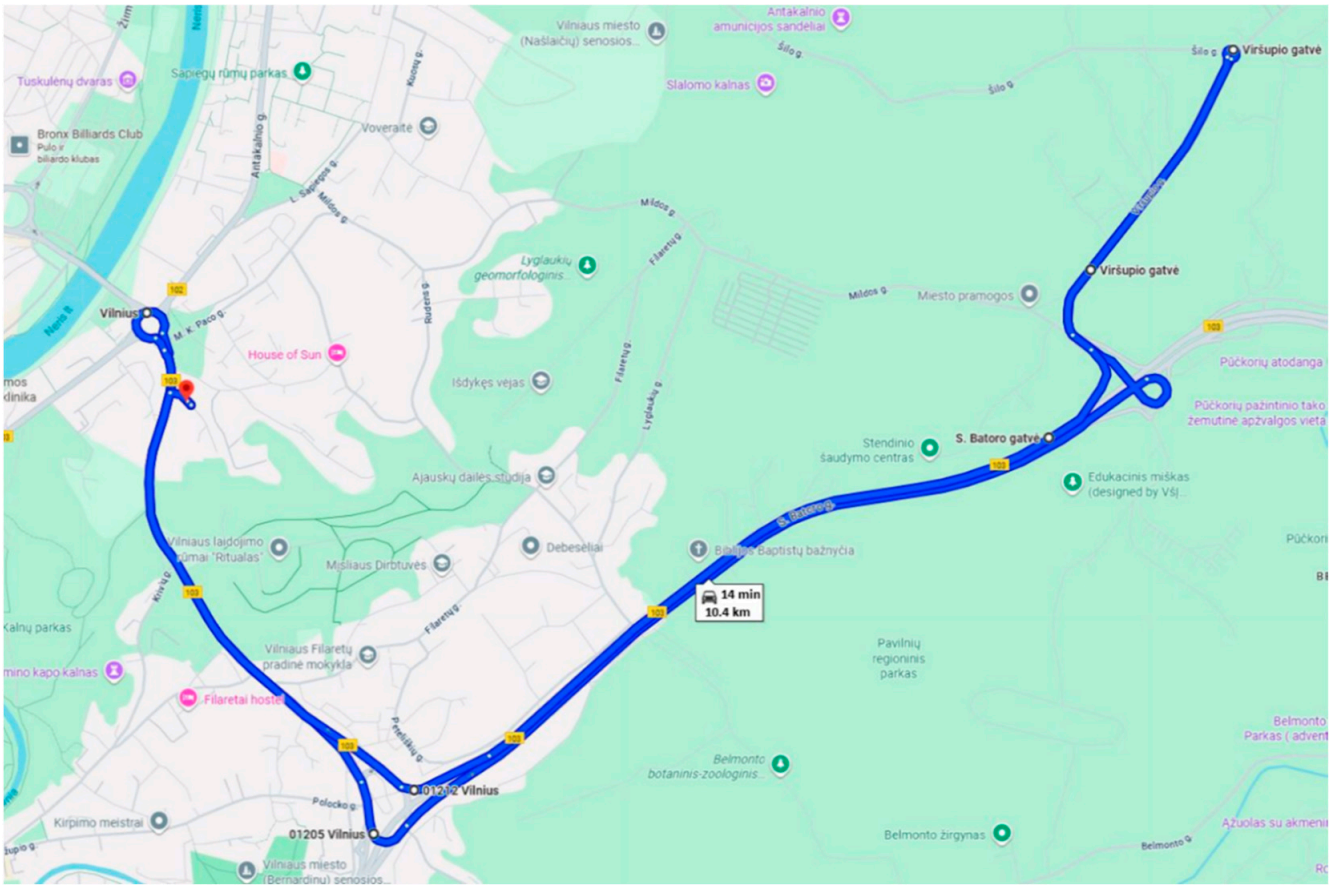


Figure 1. Test route of the vehicle in Vilnius.

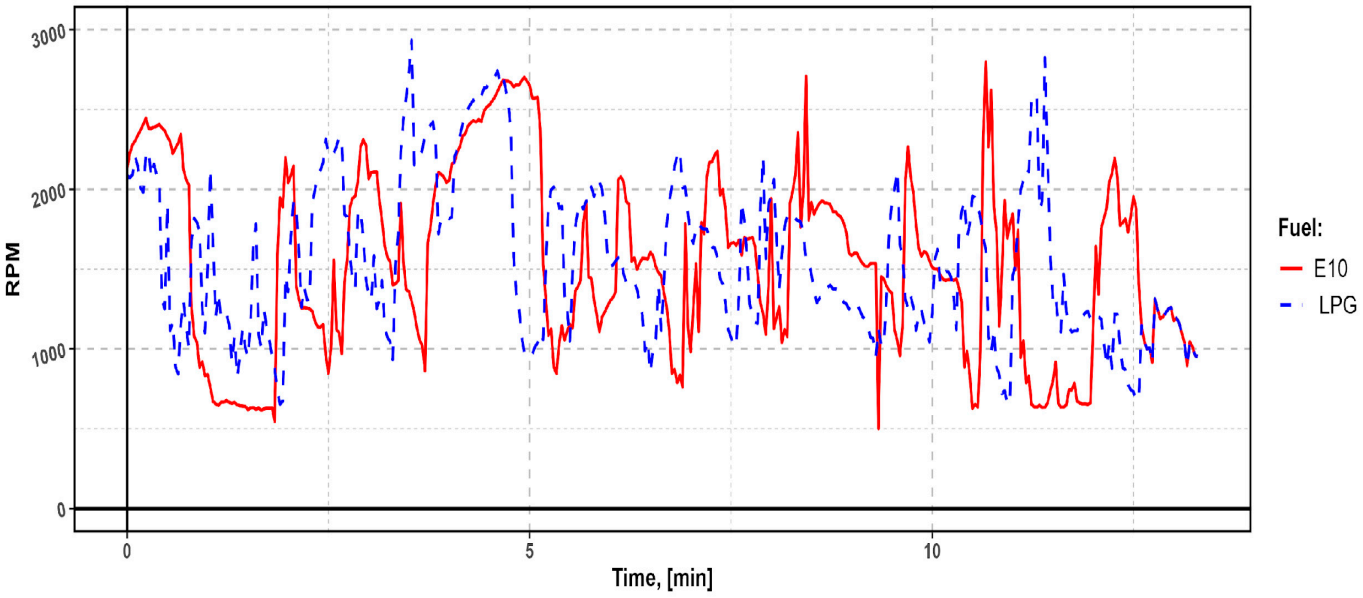


Figure 2. Vehicle driving time and engine speed (RPM).

The vehicle and engine diagnostic tool "Launch X-431 Pro" was connected via the OBD2 interface and used to record engine operating parameters during vehicle operation. Using this device, the following parameters were logged every 1 s: engine brake power (P_B, kW), engine speed (n, rpm), air mass flow (m_{air}, kg/h), and air–fuel excess ratio (λ).

Table 1. Technical specifications of the MRU "Nova Plus" gas analyser.

Measured Components	Measuring Ranges	Resolution	Accuracy
Carbon monoxide (CO)	0 . . . 4000 ppm/overload 10,000 ppm	1 ppm	±10 ppm or 5% reading < 4000 ppm/10% reading > 4000 ppm
Carbon dioxide (CO_2)	0 . . . 40 Vol %	0.1%	±0.3% or 5% of the measured value
Hydrocarbons (HC)	0 . . . 2000 ppm up to 20,000 ppm	0.1%	±30 ppm % or 3% of the measured value
Nitrogen oxides (NO_x)	0 . . . 1000 ppm/overload 5000 ppm	1 ppm	±5.0 ppm or 5% reading < 1000 ppm/10% reading > 1000 ppm

3.2. Determination of Engine Specific Emissions in a Real Driving Test

Data from the diagnostic device, and the gas analyser were also recorded every 1 s; however, prior to performing emission calculations, the data were synchronised to account for delays inherent to the exhaust and pollutant measurement systems of the gas analyser. During data synchronisation, it considered that a rapid increase in engine load leads to a corresponding rise in pollutant concentrations (e.g., CO), as the catalytic converter cannot completely neutralise the significant increase in emissions. The synchronisation procedure ensured that rapid increases in engine load coincided with the corresponding increases in pollutant concentrations.

The specific emission of exhaust gases was calculated by considering the measured volumetric concentration of each pollutant, its molar mass, the exhaust mass flow rate, the molar mass of the exhaust gases, and the engine brake power. The specific emission of carbon monoxide at each real driving point (every 1 s) was calculated using the following formula [45]:

$$E_{CO} = \frac{CO \cdot M_{CO} \cdot m_{ex}}{M_{ex} \cdot P_B \cdot 1000}, \text{ g/kWh;} \quad (1)$$

where CO—carbon monoxide concentration (ppm), measured using the "Nova Plus"; M_{CO}—molar mass of carbon monoxide, M_{CO} = 28.01 g/mol. The following molar masses were used for calculating the specific emissions of other pollutants: M_{CO_2} = 44.01 g/mol, M_{HC} = 13.09 g/mol, M_{NOx} = 32.41 g/mol; M_{ex}—total exhaust gas mass flow (kg/h), calculated using data from the "Launch X-431 Pro"; M_{ex}—molar mass of the exhaust gas mixture (g/mol), calculated based on the concentrations of individual exhaust gas components; P_B—engine brake power (kW), determined using the "Launch X-431 Pro".

Total exhaust gas mass flow:

$$m_{ex} = m_{air} + m_f, \text{kg/h;} \quad (2)$$

where m_{air}—mass flow of intake air measured during the test (kg/h), determined using the "Launch X-431 Pro"; m_f—fuel mass consumption (kg/h).

Fuel mass consumption was calculated taking into account the air flow, air–fuel excess ratio, and the air requirement for stoichiometric combustion [45]:

$$m_f = \frac{m_{air}}{\lambda \cdot A/F}, \text{kg/h;} \quad (3)$$

where λ—air–fuel excess ratio measured during the test using the "Launch X-431 Pro"; *A/F*—air-to-fuel mass ratio of the stoichiometric mixture, calculated based on the chemical composition of the fuel. For E10 fuel, λ = 14.47, and for LPG, λ = 15.77.

3.3. Analysis of Engine Workload Distribution During Tests

To compare the emissions generated by the internal combustion engine during the tests powered by different fuels, we determine the probability density function (distribution) of the engine workload. At the beginning, the workload grid has been defined in the engine load and engine speed (RPM) coordinate system. For each fuel $c \in \{E10, LPG\}$

the range of load $[L_{min}, L_{max}]$ and range of engine speed $[R_{min}, R_{max}]$ have been established, where the values $L_{min} \leq min\{L_i^c : 1 \leq i \leq n\}$, $L_{max} > max\{L_i^c : 1 \leq i \leq n\}$ and $R_{min} \leq min\{R_i^c : 1 \leq i \leq n\}$, $R_{max} > max\{R_i^c : 1 \leq i \leq n\}$ denote the highest and lowest values of load and engine speed, respectively, during the journey.

Next the load range has been divided into k separated classes (intervals) $\left[\widetilde{L}_i, \widetilde{L}_{i+1}\right)$ for $1 \leq i \leq k$, where $\widetilde{L}_1 = L_{min}, \widetilde{L}_{k+1} = L_{max}$ and the obtained classes must meet the condition $\left[\widetilde{L}_1, \widetilde{L}_1\right) \cup \left[\widetilde{L}_2, \widetilde{L}_3\right) \cup \ldots \cup \left[\widetilde{L}_k, \widetilde{L}_{k+1}\right) = [L_{mim}, L_{max})$. In a similar way the engine speed range has been devided into m separated classes, where $\left[\widetilde{R}_j, \widetilde{R}_{j+1}\right)$ for $1 \leq j \leq m$, $\widetilde{R}_1 = R_{min}$, $\widetilde{R}_{m+1} = R_{max}$ where the obtained classes satisfy the condition $\left[\widetilde{R}_1, \widetilde{R}_2\right) \cup \left[\widetilde{R}_2, \widetilde{R}_3\right) \cup \ldots \cup \left[\widetilde{R}_m, \widetilde{R}_{m+1}\right) = [R_{mim}, R_{max})$.

For each class we determine the representative, which is defined as middle of interval. From above the values $\bar{L}_i = \frac{1}{2}\left(\widetilde{L}_i + \widetilde{L}_{i+1}\right), 1 \leq i \leq k$ and $\bar{R}_i = \frac{1}{2}\left(\widetilde{R}_j + \widetilde{R}_{j+1}\right), 1 \leq j \leq m$ denotes the class representatives of load and RPM respectively. Thus, we obtain the grid $\left\{\left(\widetilde{L}_i, \widetilde{R}_j\right)\right\}_{1 \leq i \leq k, 1 \leq j \leq m}$ of engine workload. For each node of grid presented possible states of loads and RPM we estimate the pollutants and frequency being in this state during the test. The expected pollution values when engine was powered by fuel $c \in \{E10, LPG\}$ was estimated as follows:

$$v_{ij} = \frac{1}{\#D_{ij}} \sum_{i \in D_{ij}} x_i^c \tag{4}$$

and the frequency of readings:

$$n_{ij} = \frac{\#D_{ij}}{n^c}; \tag{5}$$

where the set:

$$D_{ij} = \left\{l : L_l^c \in \left[\widetilde{L}_i, \widetilde{L}_{i+1}\right), R_l^c \in \left[\widetilde{R}_j, \widetilde{R}_{j+1}\right), 1 \leq l \leq n^c\right\} \tag{6}$$

for $1 \leq i \leq k, 1 \leq j \leq m$, $\#D$ describes the cardinality of D.

The scatter plot of sequence $\left\{\left(\widetilde{L}_i, \widetilde{R}_j, v_{ij}\right)\right\}_{1 \leq i \leq k, 1 \leq j \leq m}$ in three-dimensional space means the shape and scale of pollution (pollution characteristic) caused by the engine operation due to load and speed (RPM). The 2D heatmap $\left\{\left(\widetilde{L}_i, \widetilde{R}_j, n_{ij}\right)\right\}_{1 \leq i \leq k, 1 \leq j \leq m}$ corresponds to the distribution of workload engine during the test.

3.4. Bilinear Interpolation

Let $\{(x_i, y_j)\}_{1 \leq i \leq k, 1 \leq j \leq m}$ denotes a grid $(x_1 < x_2 < \cdots < x_k, y_1 < y_2 < \cdots < y_m)$ and $\{v_{ij}\}_{1 \leq i \leq k, 1 \leq j \leq m}$ sequence of values corresponding to points on this grid. To estimate the values on the rectangular $[x_1, x_k] \times [y_1, y_m]$ the bilinear interpolation [46] has been applied. According to bilinear interpolation the function $f(x, y)$:

$$f(x, y) = \sum_{i=1}^{k-1} \sum_{j=1}^{m-1} f_{ij}(x, y) I_{([x_i, x_{i+1}] \times [y_i, y_{i+1}])}(x, y) \tag{7}$$

Allows to estimate the value at each point $(x, y) \in [x_1, x_k] \times [y_1, y_m]$, where the indicator function is equal:

$$I_{([x_i,x_{i+1}]\times[y_i,y_{i+1}])}(x,y)=\begin{cases}1, & (x,y)\in[x_i,x_{i+1}]\times[y_i,y_{i+1}],\\ 0, & (x,y)\notin[x_i,x_{i+1}]\times[y_i,y_{i+1}],\end{cases}$$

and on the rectangular $[x_i,x_{i+1}]\times[y_i,y_{i+1}]$, $1\le i\le k-1, 1\le j\le m-1$ the function:

$$f_{ij}(x,y)=\frac{1}{(x_{i+1}-x_i)(y_{i+1}-y_i)}[x_{i+1}-x,x-x_i]\begin{bmatrix}v_{ij} & v_{i,j+1}\\ v_{i+1,j} & v_{i+1,j+1}\end{bmatrix}\begin{bmatrix}y_{i+1}-y\\ y-y_i\end{bmatrix} \tag{8}$$

takes values $f(x_i,y_j)=v_{ij}$, $f(x_{i+1},y_j)=v_{i+1,j}$, $f(x_i,y_{j+1})=v_{i,j+1}$, $f(x_{i+1},y_{j+1})=v_{i+1,j+1}$ (values corresponding to the values on the grid). By applying the bilinear interpolation, we can estimate the emissions of pollutants over the entire load and speed engine range, thus on the entire rectangle $[x_1,x_k]\times[y_1,y_m]$.

The interpolation-based emission surface modelling will be used to compare the emission per revolution (called unit emission/instantaneous emission) generated by the engine in a real-time test (real conditions). To estimate the pollutant emission data-driven techniques [10,11,47] (e.g., linear or nonlinear approximation, neural networks) can be used, and these have been successfully used for diagnostic modelling. Bilinear interpolation is a very simple method for determining engine load distribution and pollutant emissions. However, data-driven techniques enable real-time emission forecasting and anomaly detection in vehicle diagnostics.

3.5. Instantaneous Emission Characteristics

In many publications, authors give emissions as the weight of pollutants divided by travelled kilometres, for tests performed on a chassis dynamometer and in real-world conditions. Unfortunately, this emission is an estimate and does not correspond to the vehicle dynamics or the engine workload. By carefully analysing the driving dynamics or engine load, we can see that pollution varies significantly under different engine operating conditions (e.g., load, RPM). The chemical properties of the fuel also affect driving dynamics and engine load. The pollution characteristics of an engine powered by fuels *Gasoline* and *LPG* has been analysed.

Under real driving conditions, the engine operating state can be specified by its instantaneous load and instantaneous RPM. Let (Ω,F,P) be a probability space. The random variables $L:\Omega\to[L_{min},L_{max}]$ and $R:\Omega\to[R_{min},R_{max}]$ denotes load and speed of the engine, respectively. Thus, the random vector $(L,R):\Omega\to[L_{min},L_{max}]\times[R_{min},R_{max}]$ determines the instantaneous state of the engine. On the other hand, the load and engine speed affect pollutant emissions. To estimate unit/instantaneous emission, we convert pollution in units [q/kWh] to [g/s] as follows:

$$\psi_i^c=\frac{L_i^c x_i^c}{3600}; \tag{9}$$

where $c\in\{E10,LPG\}$, $0\le i\le n^c$.

The main aim is to compare emissions from fuels used to power the engine. Based on sequences $\{(L_i^c,R_i^c,\psi_i^c)\}_{0\le i\le n^c}$, $c\in\{E10,LPG\}$ from formulas (4) and (5) we determine the grids $\left\{\begin{pmatrix}\overset{\sim c}{L}_i,\overset{\sim c}{R}_j,v_{ij}^c\end{pmatrix}\right\}_{1\le i\le k,1\le j\le m}$ and $\left\{\begin{pmatrix}\overset{\sim c}{L}_i,\overset{\sim c}{R}_j,n_{ij}^c\end{pmatrix}\right\}_{1\le i\le k,1\le j\le m}$, $c\in\{E10,LPG\}$. These grids correspond to the pollution characteristics and the probability density of engine operation and from Formula (8) we determine the functions $f_c(L,R)$ and $g_c(L,R)$ defining the pollution value [g/s] and the probability density of engine operation during the test

due to load and RPM. Additionally, the probability density of engine operation in the load and RPM coordinate system satisfies the condition:

$$\int_{L_{min}}^{L_{max}} \int_{R_{min}}^{R_{max}} g_c(x,y)dxdy = 1 \tag{10}$$

The density function $g_c(v,a)$ is responsible for the operation/usage of the engine during the test. According to the above the expected unit/instantaneous emission (pollution per revolution, Φ_c[g]) is estimated as follows:

$$E\Phi_c = \int_{L_{min}}^{L_{max}} \int_{R_{min}}^{R_{max}} \frac{60 f_c(l,r)}{r} g_c(l,r)dldr \tag{11}$$

for fuel type $c \in \{E10, LPG\}$. The vehicle dynamics under real-world conditions is defined by a random vector (L,R) we can calculate the dispersion of instantaneous emissions. Thus, the value

$$S^2\Phi_c = \int_{L_{min}}^{L_{max}} \int_{R_{min}}^{R_{max}} \left(\frac{60 f_c(l,r)}{r} - E\Phi_c \right)^2 g_c(l,r)dldr \tag{12}$$

denotes the variance of unit emission per revolution, but $S\Phi_c = \sqrt{S^2\Phi_c}$ standard deviation of the unit emission per revolution. The coefficient of variation [100%] of unit emission (ratio of the standard deviation to the mean) is equal:

$$\kappa_c = \frac{S\Phi_c}{E\Phi_c} 100\%. \tag{13}$$

The coefficient of variation is an assessment of assay/test quality and thus the precision of the obtained results.

To compare instantaneous emissions based on fuel type, we determine the emission ratio and the percentage increase in emissions, where as a baseline emission we take the instantaneous emission generated by an engine powered by classic $E10$ fuel. The value:

$$\lambda_{LPG/E10} = \frac{E\Phi_{LPG}}{E\Phi_{E10}} \tag{14}$$

is called the unit emission ratio generated by LPG fuel in relation to $E10$ fuel, therefore:

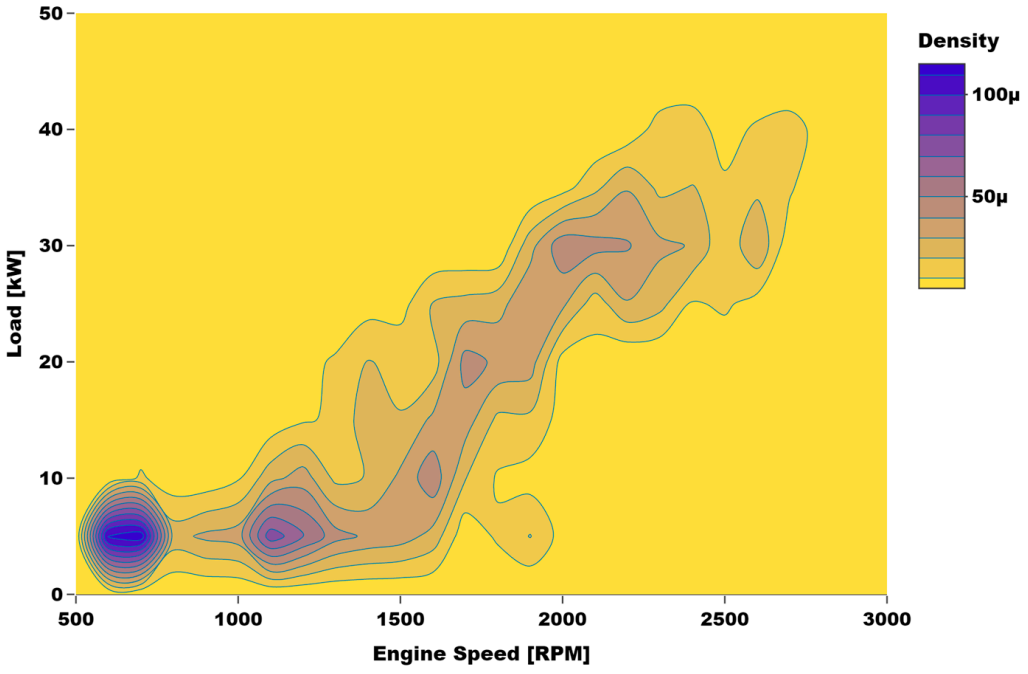
$$\beta_{LPG/E10} = (\lambda_{LPG/E10} - 1)100\% \tag{15}$$

denotes percentage increase in expected unit emission generated by LPG fuel in relation to $E10$ fuel.

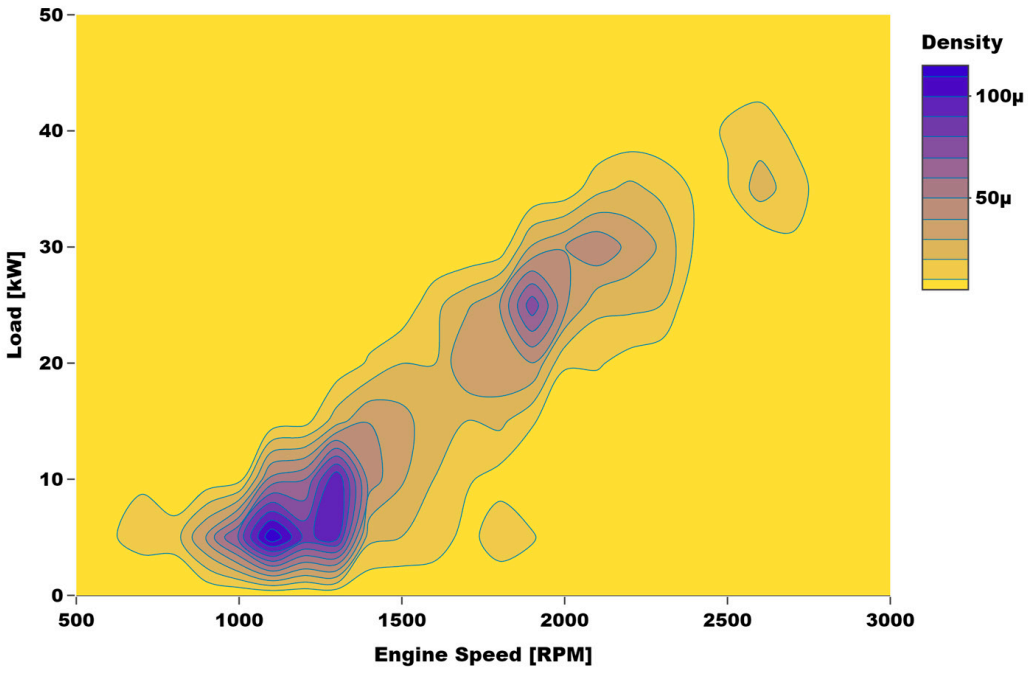
4. Results

Figure 3a,b show the joint probability density distributions of engine operating conditions (load and RPM) for urban drives using E10 and LPG fuels, respectively. In both cases, the highest probability regions align along a diagonal trajectory from low to moderate engine speed and load, indicating that most engine work occurred under typical city driving conditions. Figure 3a presents the joint probability density distribution of engine operating conditions (load and speed) during the urban drive using E10 fuel. The highest density region is concentrated at low RPM (around 700–900 RPM) and low load (~0–5 kW), indicating frequent idling or coasting events. A secondary density ridge extends diagonally toward moderate RPM (1500–2200) and loads of 10–30 kW, suggesting that most driving occurred under mild acceleration or steady-state cruising conditions. The presence

of multiple local maxima implies a variable driving pattern, reflecting realistic stop-and-go urban dynamics.



(**a**)



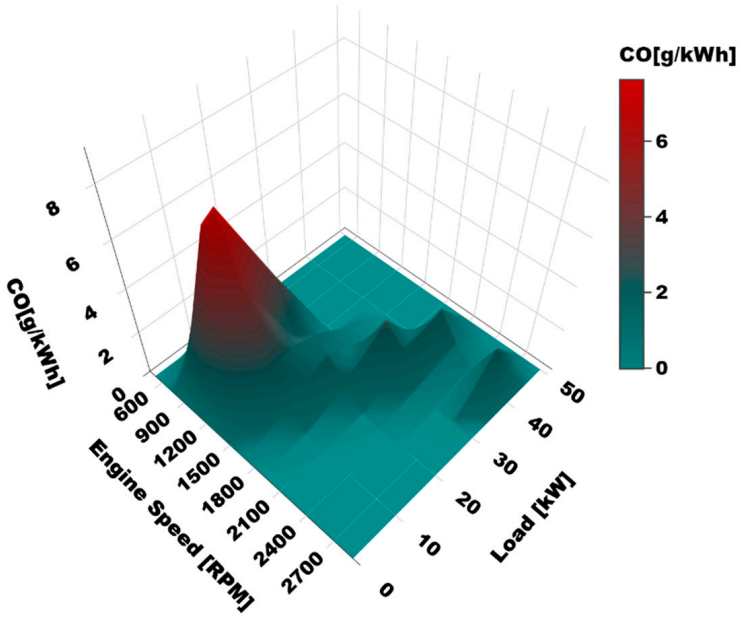
(**b**)

Figure 3. Joint probability density function of engine load and speed when fuelled with: (**a**) E10, (**b**) LPG.

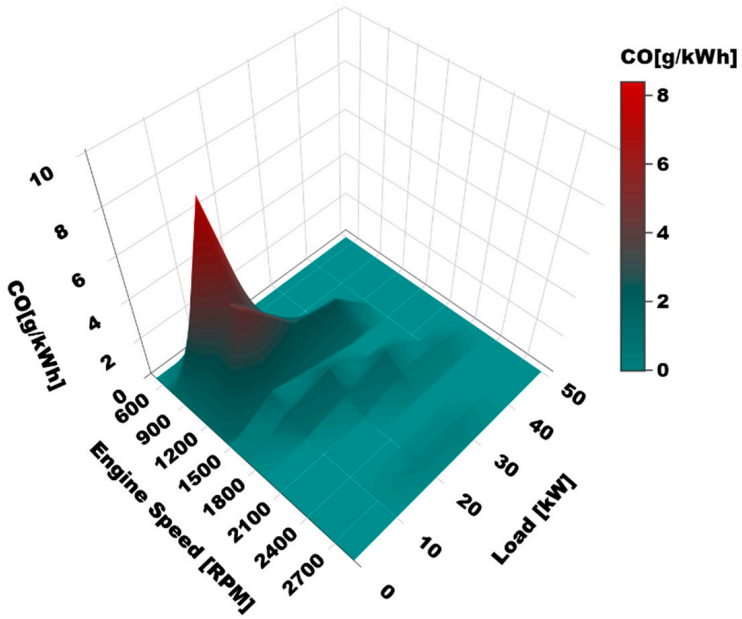
However, the LPG-fuelled drive (Figure 3b) shows a more concentrated and localised density peak around 1100–1400 RPM and 5–15 kW, suggesting steadier driving with fewer transient load conditions. In contrast, the E10 case (Figure 3a) exhibits greater dispersion toward very low and high load values, and a more substantial presence of idle operation (below 1000 RPM, under 5 kW), implying more frequent deceleration, stops or coasting events. These subtle differences in the engine's operating envelope confirm that

while the overall driving patterns were similar, the load distribution and engine utilisation varied depending on the fuel type, which must be accounted for when interpreting emission measurements.

Figure 4a presents a 3D surface map of CO emissions [g/kWh] as an engine load and speed function for the E10-fuelled drive. A distinct emission spike is observed at low engine speed (~800 RPM) and very low load, where CO emissions exceed 20 g/kWh. This peak likely corresponds to engine idling or transient deceleration phases, where incomplete combustion is more likely to occur, especially in gasoline engines. Across the rest of the load-speed spectrum, CO emissions remain significantly lower, often close to zero, indicating relatively clean combustion under moderate and high load conditions.



(**a**)



(**b**)

Figure 4. Interpolated CO emission surface [g/kWh] under urban driving conditions with the engine fuelled by: (**a**) E10, (**b**) LPG.

Figure 4a,b compare the interpolated CO emission surfaces [g/kWh] for E10 and LPG operation. While both fuels exhibit higher CO levels at low engine loads, the LPG-fuelled engine shows a noticeably stronger peak under idle conditions. Notably, the peak CO emission is significantly higher for LPG, reaching over 35 g/kWh, compared to a maximum of ~25 g/kWh for E10. This suggests that LPG combustion may be less efficient regarding CO oxidation during low-load operation, likely due to lower in-cylinder temperatures or incomplete air-fuel mixing under idle conditions. Outside this specific zone, CO emissions are minimal across the working range for both fuels. However, the elevated peak in the LPG case highlights a greater sensitivity to operating conditions (Figure 4b). It underlines the importance of engine calibration for alternative fuels, especially in low-speed urban use.

Figure 5a displays the interpolated CO_2 emission surface [g/kWh] for the engine powered by E10 during urban driving. The map reveals a broad distribution of CO_2 emission intensities across the engine's operational envelope, with the highest values (~900 g/kWh) occurring in two regions: at low RPMs (800–1200) and moderate load (10–20 kW), and higher RPMs (~1800–2400) and load above 20 kW. This bimodal pattern reflects typical combustion behaviour: under partial load, the engine may operate at suboptimal efficiency (resulting in elevated emissions per unit energy), whereas under higher load, although fuel flow increases, the specific energy output is also higher, potentially normalising the emission intensity. The smoother shape of the surface compared to the CO maps suggests more stable and predictable CO_2 production, consistent with its role as a combustion product directly proportional to fuel consumption.

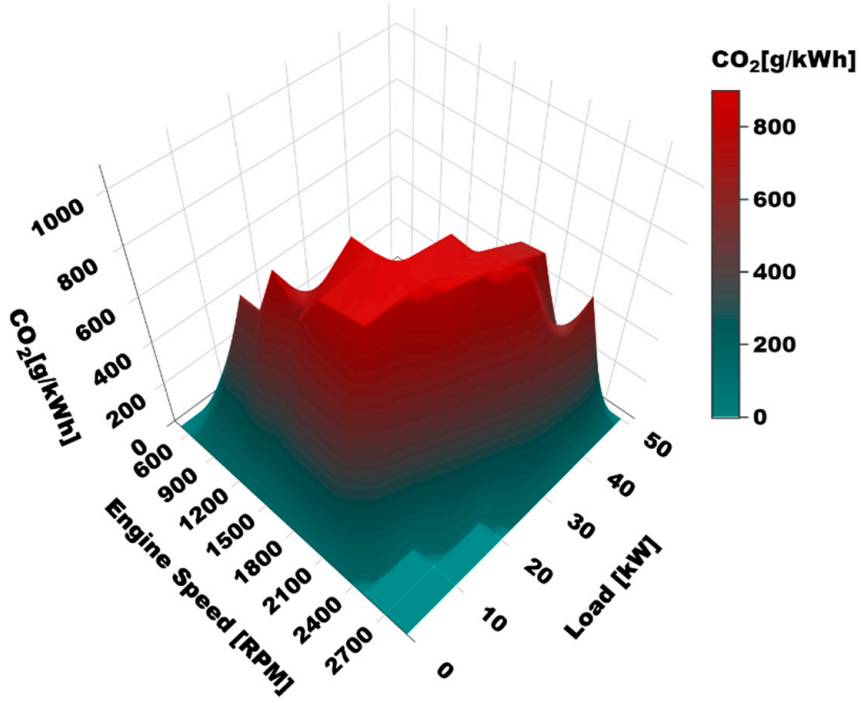
Figure 5a,b present the interpolated surfaces of CO_2 emissions [g/kWh] for the engine operating on E10 and LPG fuels, respectively. Both maps show that CO_2 emissions increase with load and engine speed, as expected, due to the higher fuel consumption required to deliver more power. The surface for E10 (Figure 5a) exhibits a more pronounced bimodal structure, with two distinct emission peaks: one at low RPM and moderate load, and another at higher RPM and high load. In contrast, the LPG-fuelled engine (Figure 5b) demonstrates a more uniform and flatter emission profile, with less variation and slightly lower peak values (~800 g/kWh vs. ~900 g/kWh for E10). This suggests that LPG combustion results in more consistent CO_2 emission rates across the operational envelope, possibly due to more homogeneous fuel-air mixing or a leaner combustion regime. The lower average CO_2 emissions for LPG, also confirmed in Table 2, support its potential as a lower-carbon alternative to gasoline in urban driving conditions.

Table 2. Parameters of unit emission of engine powered by different fuels.

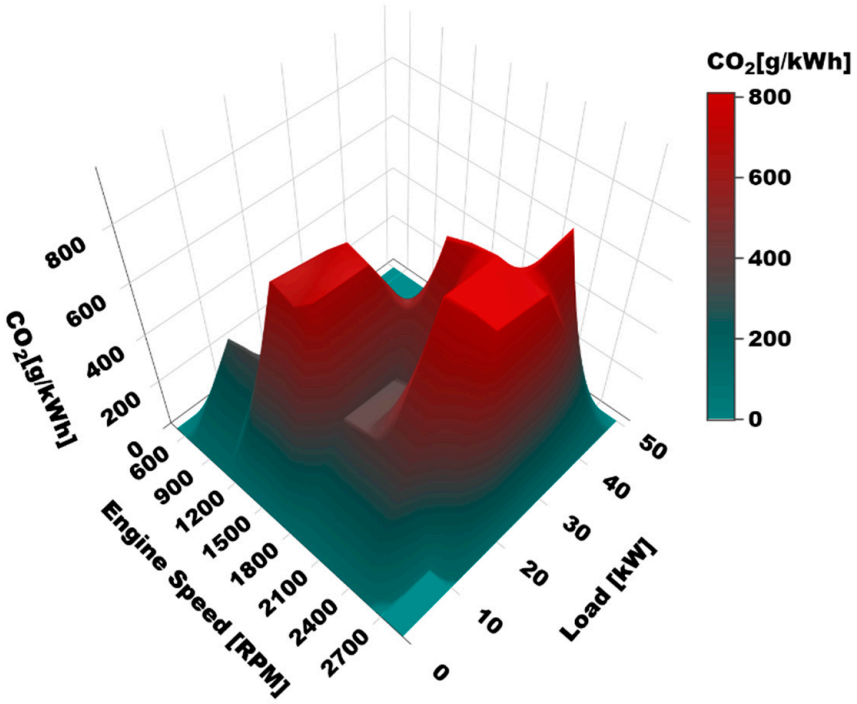
Fuel	Pollution	$E\Phi$, [mg/rev]	$S\Phi$, [mg/rev]	κ_c, [%]
E10	CO	0.221	0.374	169.54
E10	CO_2	63.717	40.951	64.27
E10	NOx	0.454	0.519	114.22
E10	HC	0.012	0.011	97.53
LPG	CO	0.242	0.540	223.36
LPG	CO_2	58.397	33.774	57.84
LPG	NOx	0.460	0.462	100.32
LPG	HC	0.013	0.010	73.83

Figure 6a presents the interpolated surface of hydrocarbon (HC) emissions [g/kWh] for the E10-fuelled engine during an urban driving test. As expected, the highest HC emissions are concentrated at low engine speed (800–1000 RPM) and minimal load (<5 kW), reaching values over 0.6 g/kWh. This region typically corresponds to idle or low-efficiency operation, where incomplete combustion and fuel quenching near cylinder walls lead to

elevated HC release. HC emissions remain low across the rest of the operating envelope, indicating that the combustion process is relatively complete under medium and high loads. The isolated nature of the emission peak suggests that the engine's aftertreatment system (if any) may be less effective during idle or cold-start conditions.

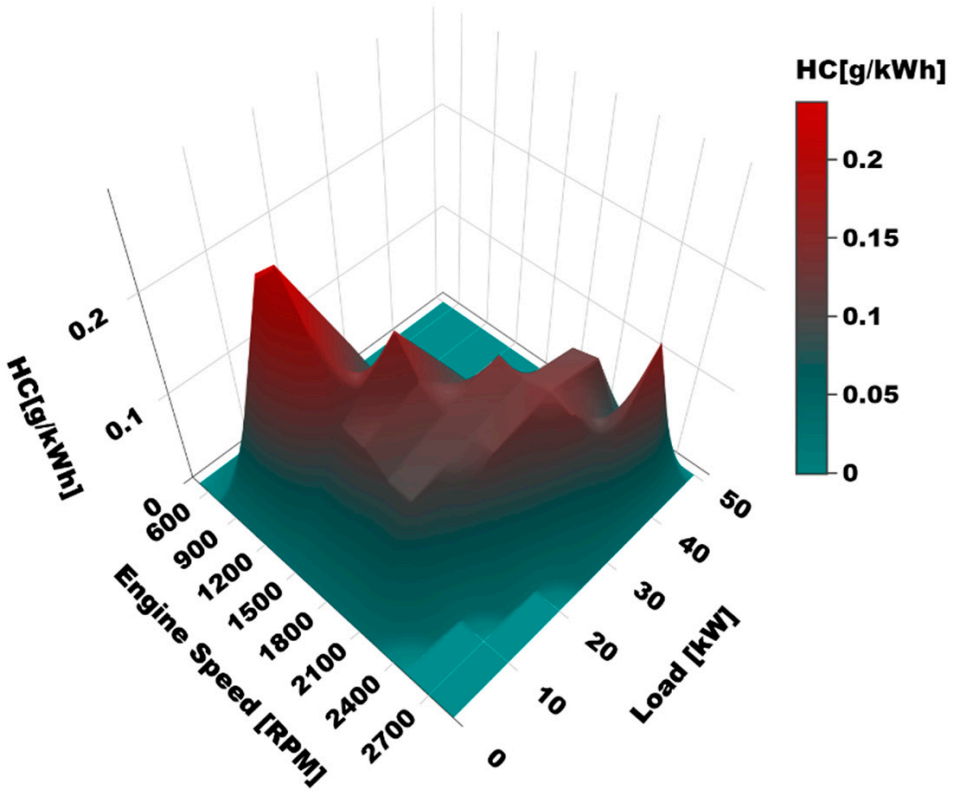


(**a**)

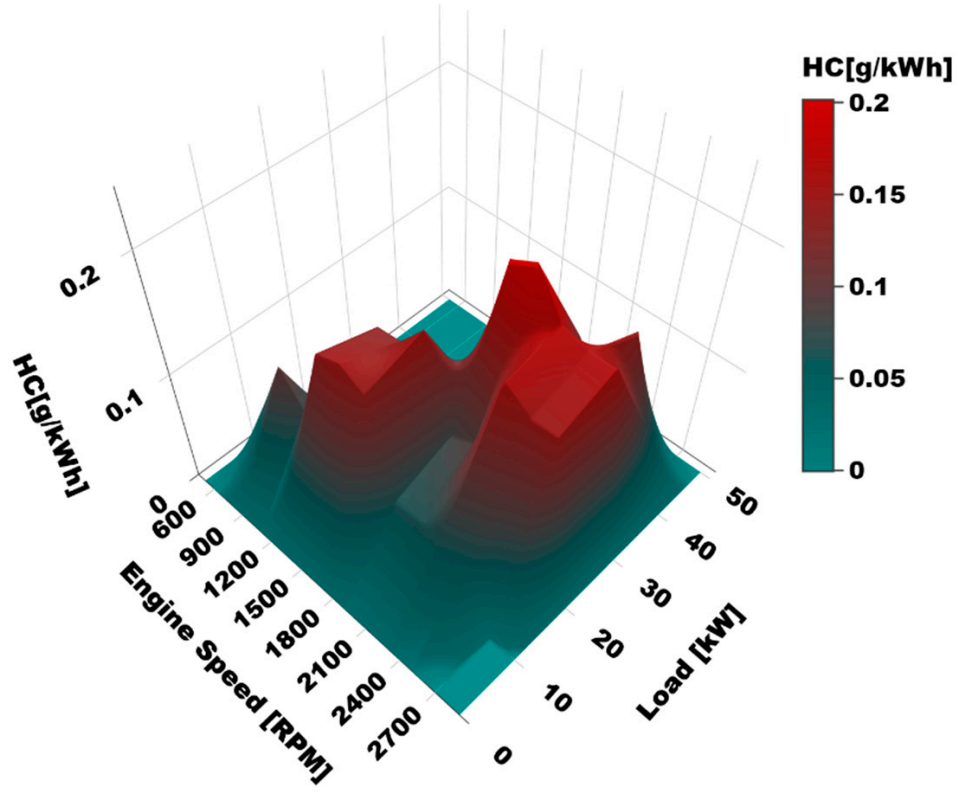


(**b**)

Figure 5. Interpolated CO_2 emission surface [g/kWh] under urban driving conditions with the engine fuelled by: (**a**) E10, (**b**) LPG.



(**a**)



(**b**)

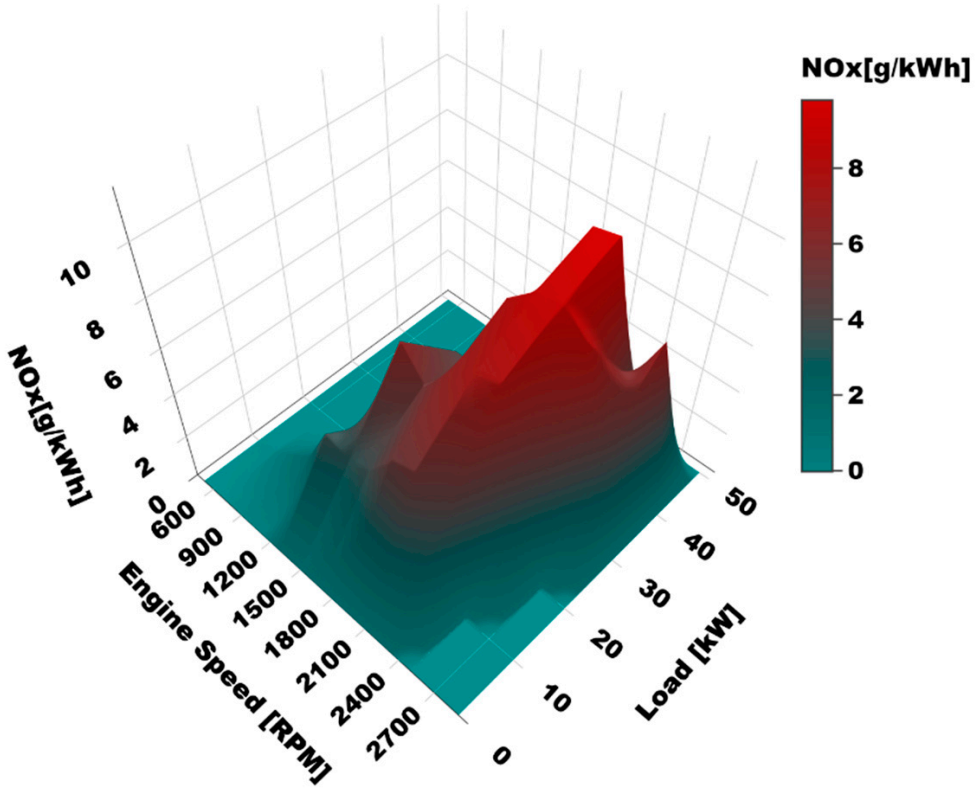
Figure 6. Interpolated HC emission surface [g/kWh] under urban driving conditions with the engine fuelled by: (**a**) E10, (**b**) LPG.

Figure 6a,b compare the interpolated HC emission surfaces [g/kWh] for the engine operating on E10 and LPG, respectively. In both cases, the highest HC emissions are observed at low RPMs (~800–1000) and low load, typical of idle and transient conditions. However, the peak value for E10 exceeds 0.6 g/kWh, while for LPG, the maximum is approximately 0.3 g/kWh—about half as much. Interestingly, the HC emission profile for LPG appears more distributed across the operational range, with non-negligible values even at moderate loads and speeds. In contrast, E10 shows a more isolated emission peak, suggesting that gasoline combustion produces a sharp HC spike only under specific low-efficiency conditions. This may reflect different flame propagation behaviour or air-fuel ratio characteristics, where LPG maintains more uniform mixing as a gaseous fuel but can lead to partial combustion under wider conditions, albeit at a lower absolute HC level.

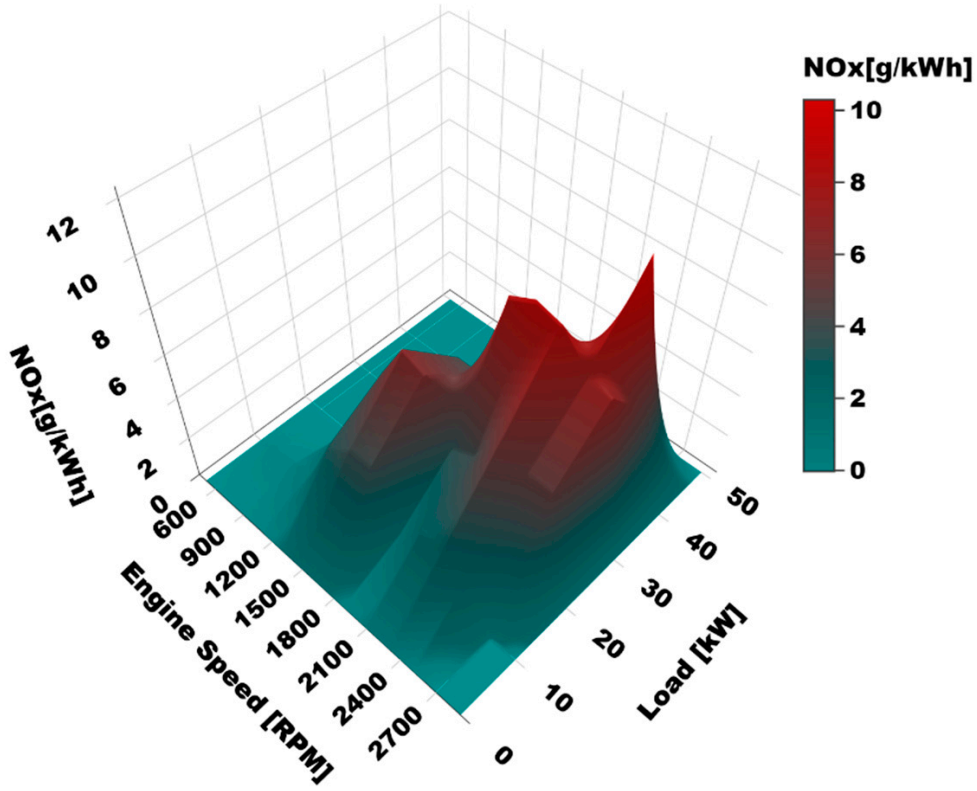
Figure 7a shows the interpolated surface of NOx emissions [g/kWh] for the engine powered by E10 during an urban driving test. The highest NOx concentrations occur in two zones: Mid-to-high engine speed (1600–2400 RPM) at medium to high load (20–40 kW), as well as a secondary peak at slightly lower speed and load (~1400 RPM, ~20 kW). This distribution is consistent with the thermal NOx formation mechanism, which intensifies at high cylinder temperatures and pressures—conditions typical during moderate-to-heavy engine load and acceleration. Unlike HC or CO, NOx emissions are negligible during idle and low-load operation. The surface shape also suggests that combustion under E10 fuel becomes less NOx-efficient once the engine enters higher-performance regimes, emphasising the need for load-sensitive emission control strategies such as EGR or aftertreatment systems.

Figure 7a,b compare the interpolated NOx emission surfaces [g/kWh] for E10 and LPG fuels. While both fuels produce NOx primarily at higher engine loads and speeds, distinct differences are observable: for E10 (Figure 7a), NOx peaks around 10 g/kWh, with two maxima: one at ~1800 RPM/25 kW and another at ~2400 RPM/35–40 kW, and for LPG (Figure 7b), the NOx surface is more concentrated and steeper, with a single dominant peak approaching 13–14 g/kWh, occurring at higher load and RPM, suggesting that LPG produces more NOx under full-load conditions. This behaviour aligns with the lean-burn characteristics of LPG, which, while improving thermal efficiency, can result in elevated combustion temperatures as a key driver of NOx formation. The absence of EGR or advanced control strategies may amplify this effect. Despite LPG's lower CO_2 footprint, its potential for higher NOx emissions under specific load regimes highlights a key trade-off that should be addressed in fuel-switching policies and calibration strategies.

Analysis of the data presented in Table 2 reveals significant differences in specific pollutant emissions characteristics depending on the fuel type. For CO, the average emission was higher for LPG, reaching 0.242 mg/rev, while for E10 it reached 0.221 mg/rev. At the same time, the coefficient of variation for LPG exceeded 220%, indicating greater data dispersion and a less stable combustion process in terms of CO emissions. For CO_2, the situation was reversed; LPG showed lower average emissions, reaching 58.397 mg/rev, representing a reduction of approximately 8.3% compared to E10 (63.717 mg/rev). Notably, the variability of these emissions was also lower, which may indicate more stable combustion of LPG in terms of CO_2 emissions. Nitrogen oxide (NOx) emissions for both fuels were very similar—an average of 0.454 mg/rev for E10 and 0.460 mg/rev for LPG. However, it is worth noting that LPG had a slightly lower standard deviation, which may suggest a more predictable NOx emission pattern, especially under higher engine load conditions. For HC, average emissions were virtually identical: 0.012 mg/rev for E10 and 0.013 mg/rev for LPG. At the same time, the coefficient of variation for LPG was lower, indicating more uniform combustion of the gaseous fuel in this range.



(**a**)



(**b**)

Figure 7. Interpolated NOx emission surface [g/kWh] under urban driving conditions with the engine fuelled by: (**a**) E10, (**b**) LPG.

Several significant differences can be identified when comparing the results of the specific pollutant emissions for E10 and LPG fuels. From a greenhouse gas emissions perspective, LPG is the more favourable fuel, generating approximately 8.35% less CO_2 per crankshaft revolution. Lower CO_2 emissions suggest higher energy efficiency or better carbon balance properties for LPG. On the other hand, LPG combustion results in higher emissions of incomplete combustion products, such as CO and HC. This may indicate lower combustion temperatures in specific load ranges, suboptimal ignition timing, or imperfect fuel-air mixing, especially under partial load conditions. Such phenomena are typical for gaseous alternative fuels, which require precise combustion process control, especially at low fuel rates. Nitrogen oxide (NOx) emissions remain similar for both fuels, but LPG exhibits a more pronounced single emission peak at full load, which can lead to higher instantaneous NOx values. This is confirmed by the map in Figure 7b, where NOx emissions for LPG exceed those for E10 under high load and rpm conditions. This phenomenon is due to the lean combustion conditions typical of LPG, which promote an increase in combustion chamber temperature—a key factor in NOx formation.

A comparison of the relative specific emissions presented in Table 3 reveals several significant differences between fuelling the engine with E10 gasoline and LPG. For carbon monoxide (CO), a value of λ(LPG/E10) = 1.095 indicates that the LPG-fuelled engine emitted approximately 9.5% more CO per crankshaft revolution than when fuelled with E10. This result is consistent with the observed higher CO emission peaks at low load and idle, suggesting less efficient oxidation under these conditions. Carbon dioxide (CO_2) results are different, with significantly lower emissions for LPG. A value of 0.9165 corresponds to an 8.35% reduction compared to gasoline, confirming the lower carbon intensity of LPG combustion and a more favourable greenhouse gas balance. For nitrogen oxides (NOx), the differences between the fuels were minimal, with LPG showing only 1.32% higher specific emissions than E10. This slight increase can be explained by the tendency of LPG to generate slightly more NOx under full-load conditions and higher combustion temperatures, while maintaining similar values in typical city driving. For hydrocarbons (HC), an 8.33% increase was recorded for LPG, which can be attributed to incomplete combustion and quenching effects, particularly during transients or idling. Overall, the results point to a characteristic trade-off: LPG reduces CO_2 emissions, which is its climatic advantage, but it can also lead to higher emissions of incomplete combustion products (CO and HC), while NOx emissions remain similar for both fuels in practice.

Table 3. Relative characteristics of unit emission due to fuels.

Pollution Type	$\lambda_{LPG/E10}$	$\beta_{LPG/E10}$ [%]
CO	1.0950	9.50
CO_2	0.9165	−8.35
NOx	1.0132	1.32
HC	1.0833	8.33

5. Discussion

Analysis of the results obtained in real-world tests indicates that replacing E10 gasoline with LPG leads to significant differences in the specific emission profile. The most pronounced effect was the reduction in carbon dioxide emissions, which, on a particular basis (mg/rev), was on average 8.35% lower for LPG than for gasoline. This confirms literature observations that LPG, due to its lower carbon content per unit of energy, systematically reduces CO_2 emissions in both chassis dynamometer tests and RDE measurements [1–3]. This reduction has significant climate impacts, as reflected in life-cycle analyses, indicating a lower total carbon footprint of LPG-powered vehicles than gasoline-powered

vehicles [34,48]. A different trend was observed for carbon monoxide: specific CO emissions were approximately 9.5% higher for LPG. This result is consistent with some field studies, which indicate a greater susceptibility of LPG-fuelled systems to CO emissions under idling and low load conditions [17,22]. This phenomenon may be related to the limited efficiency of the combustion process at low engine speeds, which favours incomplete fuel oxidation.

On the other hand, numerous examples of significant CO reductions in LPG vehicles compared to gasoline, reaching 30–60%, are also reported in the literature [25,26]. These differences indicate a strong dependence on the fuel technology, engine control strategy, and the age and technical condition of the vehicle. Hydrocarbon (HC) emissions were characterised by an average specific emission rate of 8.3% higher when fuelled with LPG. At the same time, spatial analysis of the emissions revealed a more uniform HC distribution across the load-speed spectrum, with lower local peaks than for gasoline. These results are consistent with observations that LPG reduces emissions of aromatics and olefins with high ozone formation potential, but may promote emissions of simple alkanes [30]. Consequently, the ozone formation potential (OFP) of LPG vehicle emissions is typically lower than that of gasoline, even though total THC levels are not always reduced. This indicates that the environmental significance of hydrocarbon emissions depends not only on their quantity but also on their chemical composition. Nitrogen oxide emissions showed minor differences between the two fuels: specific NOx values for LPG were 1.3% higher on average. This result is within the measurement error and should be considered a result dependent on specific operating conditions. The literature provides both examples of increased NOx emissions when fuelled with LPG, attributed to higher combustion temperatures [17], and reports of their reduction, particularly in two-stroke engines and lean-burn applications [28]. The ultimate effect, therefore, remains a function of the ignition control strategy, combustion thermal characteristics, and engine load.

The test results confirmed the significant role of engine operating parameters in shaping the emission profile. Analysis of the load-speed system revealed that LPG promotes more frequent steady-state conditions at low and medium loads, which translates into CO_2 emission stability and reduced fluctuations. At the same time, increased CO and HC emissions were recorded in the low-load and idle regions, highlighting the importance of this engine operating range for the overall emission balance. Similar observations were presented in comparative studies of specific emissions under real-world conditions [20,49], indicating that engine load is a decisive factor for instantaneous emission levels.

The issue of assessment methodology requires a separate discussion. Based on g/km indices, the traditional approach does not reveal the impact of varying engine operating conditions between different fuels. This analysis utilises an emission unit related to crankshaft rotation (mg/rev) and bilinear interpolation in the load-RPM space. This approach enabled the identification of critical areas of engine operation and captures differences that remain invisible in a distance-based approach. These differences are significant when analysing alternative fuels, where emission levels and the distribution of engine operating conditions change. The results indicate the need to integrate specific emission methodologies and operating state distributions in comparative fuel studies, a finding confirmed by recent studies on instantaneous emissions [41,50]. In summary, the applied methodology allowed for an objective comparison of LPG and gasoline emissions under real-world operating conditions, revealing the benefits of CO_2 and PN/PM reductions and the challenges associated with CO and HC emissions at low loads. The results indicate the need for further optimisation of combustion strategies and calibration of LPG fuel systems to maximise the environmental benefits of this fuel.

6. Conclusions

Real-world urban driving tests using a Subaru Outback III AWD, fuelled alternately with E10 gasoline and LPG, allowed for a more in-depth assessment of the impact of fuel type on engine performance and pollutant emissions. Advanced methodology, including synchronous recording of engine operating parameters and exhaust gas concentrations and calculations of specific emissions relative to crankshaft rotation, allowed for the detection of subtle differences that would not be visible in a traditional analysis per kilometre of mileage. Supplementing the analysis with bilinear interpolation in the load-RPM space allowed for the reconstruction of emission surfaces and identifying the most critical engine operating areas for individual pollutant emissions.

The results indicate that LPG has a significantly lower carbon dioxide emission intensity, with an average reduction of 8.3% compared to E10 gasoline, confirming this fuel's more favourable carbon properties and its potential for reducing greenhouse gas emissions. At the same time, however, an increase in emissions of incomplete combustion products was observed: for carbon monoxide by an average of 9.5% and for hydrocarbons by 8.3%. Higher CO emission peaks were particularly noticeable during idle and low-load conditions when fuelled with LPG, indicating less efficient oxidation processes. For hydrocarbons, LPG had a beneficial effect on lower peak values than gasoline. Still, their distribution throughout the engine's operating range proved more even, suggesting particular susceptibility to incomplete combustion even at moderate loads. NOx emissions remained similar for both fuels, with an average difference of only 1.3%. However, LPG generated a steeper peak under high-load and higher engine speed conditions, consistent with lean combustion characteristics and increased combustion chamber temperatures. The overall assessment thus points to a characteristic compromise in LPG use: on the one hand, clear climate benefits in the form of CO_2 reduction; on the other, increased emissions of incomplete combustion products, requiring the further optimisation of combustion strategies and fuel system calibration. The analytical methodology used proved to be an effective tool, allowing for precise comparisons of different fuels and identifying specific areas of engine operation that determine the emission balance. The research results can provide a basis for improving engine control algorithms in LPG-powered vehicles to fully utilise the environmental potential of this fuel while minimising its weaknesses.

Author Contributions: Conceptualization, E.K., A.R., P.W. and P.L.; methodology, E.K., A.R., M.Z.-L., P.W., M.T., P.L. and R.M.; software, E.K. and M.T.; validation, E.K., M.T. and R.M.; formal analysis, E.K., A.R., M.Z.-L., J.M., P.W., P.L. and R.M.; investigation, E.K., A.R., M.Z.-L., J.M., P.W. and P.L.; resources, M.Z.-L. and P.L.; data curation, A.R. and P.W.; writing—original draft preparation, E.K., A.R., M.Z.-L., J.M. and P.L.; writing—review and editing, M.Z.-L., J.M., P.W. and R.M.; visualization, E.K. and M.T., supervision, M.Z.-L., P.W., M.T. and R.M.; project administration, A.R., M.Z.-L. and J.M.; funding acquisition, A.R. and J.M. All authors have read and agreed to the published version of the manuscript.

Funding: This research received no external funding.

Data Availability Statement: Data are available after request to the corresponding author.

Acknowledgments: This article is based on research conducted during the scientific internship of Magdalena Zimakowska-Laskowska at the Vilnius Tech Mechanical Science Institute, held from 25 November to 24 December 2024.

Conflicts of Interest: Author Magdalena Zimakowska-Laskowska and Piotr Wiśniowski were employed by the Environment Protection Centre. The remaining authors declare that the research was conducted in the absence of any commercial or financial relationships that could be construed as a potential conflict of interest.

Abbreviations

CO	Carbon monoxide
CO_2	Carbon dioxide
E10	Gasoline blend containing 90% gasoline and 10% bioethanol (by volume)
$E\Phi$	Instantaneous emission
HC	Hydrocarbons
LHV	Lower heating value
LPG	Liquefied Petroleum Gas
NOx	Nitrogen oxides
OBD	On-Board Diagnostics
RDE	Real Driving Emissions
RPM	Engine speed as measured in Revolutions Per Minute
$S\Phi$	Dispersion of instantaneous emission
$\beta_{LPG/E10}$	Percentage increase of emissions
κ	Coefficient of variation
λ	Air–fuel excess ratio
$\lambda_{LPG/E10}$	Emission ratio

References

1. Lyu, M.; Xu, Y.; Huang, M.; Wang, Y. Real World Emissions in a High-Altitude City: A Comparison between LPG Taxis and Gasoline Cars. In Proceedings of the WCX SAE World Congress Experience, Detroit, MI, USA, 8–10 April 2025.
2. Šarkan, B.; Jaśkiewicz, M.; Kubiak, P.; Tarnapowicz, D.; Loman, M. Exhaust Emissions Measurement of a Vehicle with Retrofitted LPG System. *Energies* **2022**, *15*, 1184. [CrossRef]
3. Bellin, T.; Casadei, S.; Rossi, T.; Bernetti, A.; De Lauretis, R.; Lonati, G. Determination of Euro 6 LPG Passenger Car Emission Factors through Laboratory and On-Road Tests: Effect on Nation-Wide Emissions Assessment for Italy. *Atmos. Environ. X* **2022**, *15*, 100186. [CrossRef]
4. Zimakowska-Laskowska, M.; Kozłowski, E.; Laskowski, P.; Wiśniowski, P.; Świderski, A.; Orynycz, O. Vehicle Exhaust Emissions in the Light of Modern Research Tools: Synergy of Chassis Dynamometers and Computational Models. *Combust. Engines* **2025**, *200*, 145–154. [CrossRef]
5. Kozłowski, E.; Borucka, A.; Oleszczuk, P.; Leszczyński, N. Evaluation of Readiness of the Technical System Using the Semi-Markov Model with Selected Sojourn Time Distributions. *Eksploat. I Niezawodn. Maint. Reliab.* **2024**, *26*, 191545. [CrossRef]
6. Oszczypała, M.; Ziółkowski, J.; Małachowski, J. Semi-Markov Approach for Reliability Modelling of Light Utility Vehicles. *Eksploat. I Niezawodn. Maint. Reliab.* **2023**, *25*, 161859. [CrossRef]
7. Grabski, F. *Semi-Markov Processes: Applications in System Reliability and Maintenance*; Elsevier: Amsterdam, The Netherlands, 2014.
8. Kozłowski, E.; Wiśniowski, P.; Gis, M.; Zimakowska-Laskowska, M.; Borucka, A. Vehicle Acceleration and Speed as Factors Determining Energy Consumption in Electric Vehicles. *Energies* **2024**, *17*, 4051. [CrossRef]
9. Tomiło, P. Classification of the Condition of Pavement with the Use of Machine Learning Methods. *Transp. Telecommun. J.* **2023**, *24*, 158–166. [CrossRef]
10. Kłosowski, G.; Rymarczyk, T.; Niderla, K.; Kulisz, M.; Skowron, Ł.; Soleimani, M. Using an LSTM Network to Monitor Industrial Reactors Using Electrical Capacitance and Impedance Tomography—A Hybrid Approach. *Eksploat. I Niezawodn. Maint. Reliab.* **2023**, *25*, 11. [CrossRef]
11. Pawlik, P.; Kania, K.; Przysucha, B. Fault Diagnosis of Machines Operating in Variable Conditions Using Artificial Neural Network Not Requiring Training Data from a Faulty Machine. *Eksploat. I Niezawodn. Maint. Reliab.* **2023**, *25*, 168109. [CrossRef]
12. Sobaszek, Ł.; Piasecka, I.; Flizikowski, J.; Tomporowski, A.; Sokolovskij, E.; Bałdowska-Witos, P. Environmentally Oriented Analysis of Benefits and Expenditures in the Life Cycle of a Wind Power Plant. *Materials* **2023**, *16*, 538. [CrossRef]
13. Hastie, T.; Tibshirani, R.; Friedman, J. *The Elements of Statistical Learning*; Springer Series in Statistics; Springer: New York, NY, USA, 2009; ISBN 978-0-387-84857-0.
14. James, G.; Witten, D.; Hastie, T.; Tibshirani, R. *An Introduction to Statistical Learning: With Applications in R*; Springer Texts in Statistics; Springer: New York, NY, USA, 2021; ISBN 978-1-0716-1417-4.
15. Rimkus, A.; Kozłowski, E.; Vipartas, T.; Pukalskas, S.; Wiśniowski, P.; Matijošius, J. Emission Characteristics of Hydrogen-Enriched Gasoline Under Dynamic Driving Conditions. *Energies* **2025**, *18*, 1190. [CrossRef]
16. Warguła, Ł.; Nati, C.; Wieczorek, B.; Bembenek, M. The Carbon Dioxide Emission Balance and Ability to Chip Wood by 10 kW Machines Used in Urban Areas in Terms of Increasing Interest in Using Wood Biomass Resources for Personal Use. *Adv. Sci. Technol. Res. J.* **2025**, *19*, 402–416. [CrossRef]

17. Talib Hashem, G.; Al-Dawody, M.F.; Sarris, I.E. The Characteristics of Gasoline Engines with the Use of LPG: An Experimental and Numerical Study. *Int. J. Thermofluids* **2023**, *18*, 100316. [CrossRef]
18. Ristovski, Z.D.; Jayaratne, E.R.; Morawska, L.; Ayoko, G.A.; Lim, M. Particle and Carbon Dioxide Emissions from Passenger Vehicles Operating on Unleaded Petrol and LPG Fuel. *Sci. Total Environ.* **2005**, *345*, 93–98. [CrossRef] [PubMed]
19. Manko, I.; Shuba, Y.; Korpach, A.; Gutarevyc, S.; Ragulskiene, J.; Pauliukas, A. Measurement of Fuel Consumption and Harmful Emissions of Cars When Using Different Types of Fuel. *J. Meas. Eng.* **2020**, *8*, 182–196. [CrossRef]
20. Kontses, A.; Triantafyllopoulos, G.; Ntziachristos, L.; Samaras, Z. Particle Number (PN) Emissions from Gasoline, Diesel, LPG, CNG and Hybrid-Electric Light-Duty Vehicles under Real-World Driving Conditions. *Atmos. Environ.* **2020**, *222*, 117126. [CrossRef]
21. Lou, D.; Qi, B.; Zhang, Y.; Fang, L. Research on the Emission Characteristics of a Passenger Car Powered by Ethanol, Methanol, and Liquefied Petroleum Gas Under Real-World Running Conditions. *J. Energy Resour. Technol.* **2023**, *145*, 042303. [CrossRef]
22. Špička, L.; Poul, A.; Huzlík, J.; Bucková, M.; Hegrová, J.; Ličbinský, R. Comparison of High Mileage LPG Cars in Different Technical Condition in Czechia: Particle-Bound PAHs. *Atmos. Environ. X* **2024**, *23*, 100294. [CrossRef]
23. Chikhi, S.; Boughedaoui, M.; Kerbachi, R.; Joumard, R. On-Board Measurement of Emissions from Liquefied Petroleum Gas, Gasoline and Diesel Powered Passenger Cars in Algeria. *J. Environ. Sci.* **2014**, *26*, 1651–1659. [CrossRef]
24. Simsek, S.; Uslu, S. Investigation of the Impacts of Gasoline, Biogas and LPG Fuels on Engine Performance and Exhaust Emissions in Different Throttle Positions on SI Engine. *Fuel* **2020**, *279*, 118528. [CrossRef]
25. Duy, V.N.; Duc, K.N.; Van, N.C. Real-Time Driving Cycle Measurements of Fuel Consumption and Pollutant Emissions of a Bi-Fuel LPG-Gasoline Motorcycle. *Energy Convers. Manag. X* **2021**, *12*, 100135. [CrossRef]
26. Chłopek, Z.; Lasocki, J.; Sar, H. Study of Dynamic and Ecological Properties of Automotive Bi-Fuel Engine. *Int. J. Energy Environ. Eng.* **2022**, *13*, 1–10. [CrossRef]
27. Aosaf, M.R.; Wang, Y.; Du, K. Comparison of the Emission Factors of Air Pollutants from Gasoline, CNG, LPG and Diesel Fueled Vehicles at Idle Speed. *Environ. Pollut.* **2022**, *305*, 119296. [CrossRef] [PubMed]
28. Usman, M.; Ijaz Malik, M.A.; Ranjha, Q.A.; Arif, W.; Jamil, M.K.; Miran, S.; Siddiqui, S. Experimental Assessment of Performance, Emission and Lube Oil Deterioration Using Gasoline and LPG for a Sustainable Environment. *Case Stud. Therm. Eng.* **2023**, *49*, 103300. [CrossRef]
29. Iodice, P.; Amoresano, A.; Langella, G. A Review on the Effects of Ethanol/Gasoline Fuel Blends on NOX Emissions in Spark-Ignition Engines. *Biofuel Res. J.* **2021**, *8*, 1465–1480. [CrossRef]
30. Guo, H.; Zou, S.C.; Tsai, W.Y.; Chan, L.Y.; Blake, D.R. Emission Characteristics of Nonmethane Hydrocarbons from Private Cars and Taxis at Different Driving Speeds in Hong Kong. *Atmos. Environ.* **2011**, *45*, 2711–2721. [CrossRef]
31. Organ, B.; Huang, Y.; Zhou, J.L.; Surawski, N.C.; Yam, Y.-S.; Mok, W.-C.; Hong, G. A Remote Sensing Emissions Monitoring Programme Reduces Emissions of Gasoline and LPG Vehicles. *Environ. Res.* **2019**, *177*, 108614. [CrossRef]
32. Zhang, Y.; Yang, W.; Simpson, I.; Huang, X.; Yu, J.; Huang, Z.; Wang, Z.; Zhang, Z.; Liu, D.; Huang, Z.; et al. Decadal Changes in Emissions of Volatile Organic Compounds (VOCs) from on-Road Vehicles with Intensified Automobile Pollution Control: Case Study in a Busy Urban Tunnel in South China. *Environ. Pollut.* **2018**, *233*, 806–819. [CrossRef]
33. Ianniello, R.; Di Blasio, G.; Marialto, R.; Beatrice, C.; Cardone, M. Assessment of Direct Injected Liquefied Petroleum Gas-Diesel Blends for Ultra-Low Soot Combustion Engine Application. *Appl. Sci.* **2020**, *10*, 4949. [CrossRef]
34. Kim, M.J.; Lee, E.J.; Kim, C.-J.; Hong, U.G.; Park, D.S.; Shin, H.; Lee, K.-Y. Life Cycle Assessment of LPG and Diesel Vehicles in Korea. *Korean J. Chem. Eng.* **2021**, *38*, 938–944. [CrossRef]
35. Giechaskiel, B.; Lähde, T.; Clairotte, M.; Suarez-Bertoa, R.; Valverde, V.; Melas, A.D.; Selleri, T.; Bonnel, P. Emissions of Euro 6 Mono- and Bi-Fuel Gas Vehicles. *Catalysts* **2022**, *12*, 651. [CrossRef]
36. Ajuka, L.O.; Kazeem, R.A.; Kuti, O.A.; Jen, T.C.; Afolalu, A.S.; Akinlabi, E.T. Decarbonized Automotive Fuel: Liquefied Petroleum Gas Biosynthesis, Benefits and Drawbacks. *Results Eng.* **2024**, *21*, 101889. [CrossRef]
37. Wang, X.; Song, G.; Zhai, Z.; Wu, Y.; Yin, H.; Yu, L. Effects of Vehicle Load on Emissions of Heavy-Duty Diesel Trucks: A Study Based on Real-World Data. *Int. J. Environ. Res. Public Health* **2021**, *18*, 3877. [CrossRef] [PubMed]
38. Kean, A.J.; Harley, R.A.; Kendall, G.R. Effects of Vehicle Speed and Engine Load on Motor Vehicle Emissions. *Environ. Sci. Technol.* **2003**, *37*, 3739–3746. [CrossRef]
39. Lu, Y.; Fan, C.; Liu, Y.; Pei, Y. Effects of Speed Extension on PCCI Combustion and Emissions in a Heavy-Duty Diesel Engine at Medium Load. *Fuel* **2022**, *313*, 123048. [CrossRef]
40. Seo, J.; Yun, B.; Park, J.; Park, J.; Shin, M.; Park, S. Prediction of Instantaneous Real-World Emissions from Diesel Light-Duty Vehicles Based on an Integrated Artificial Neural Network and Vehicle Dynamics Model. *Sci. Total Environ.* **2021**, *786*, 147359. [CrossRef]
41. Qiu, M.; Borken-Kleefeld, J. Using Snapshot Measurements to Identify High-Emitting Vehicles. *Environ. Res. Lett.* **2022**, *17*, 044045. [CrossRef]

42. Davison, J.; Bernard, Y.; Borken-Kleefeld, J.; Farren, N.J.; Hausberger, S.; Sjödin, Å.; Tate, J.E.; Vaughan, A.R.; Carslaw, D.C. Distance-Based Emission Factors from Vehicle Emission Remote Sensing Measurements. *Sci. Total Environ.* **2020**, *739*, 139688. [CrossRef]
43. Chen, Y.; Ma, J.; Han, B.; Zhang, P.; Hua, H.; Chen, H.; Su, X. Emissions of Automobiles Fueled with Alternative Fuels Based on Engine Technology: A Review. *J. Traffic Transp. Eng. Engl. Ed.* **2018**, *5*, 318–334. [CrossRef]
44. Teixeira, A.C.R.; Machado, P.G.; Collaço, F.M.D.A.; Mouette, D. Alternative Fuel Technologies Emissions for Road Heavy-Duty Trucks: A Review. *Environ. Sci. Pollut. Res.* **2021**, *28*, 20954–20969. [CrossRef]
45. Heywood, J.B. *Internal Combustion Engine Fundamentals*, 2nd ed.; McGraw-Hill Education: New York, NY, USA, 2018; ISBN 978-1-260-11610-6.
46. Riccardi, G.; Cifra, B.A.; De Bernardis, E. *Multidimensional Differential and Integral Calculus: A Practical Approach*; Springer Nature: Cham, Switzerland, 2024; ISBN 978-3-031-70325-6.
47. Wójcik, D.; Rymarczyk, T.; Przysucha, B.; Gołąbek, M.; Majerek, D.; Warowny, T.; Soleimani, M. Energy Reduction with Super-Resolution Convolutional Neural Network for Ultrasound Tomography. *Energies* **2023**, *16*, 1387. [CrossRef]
48. Boureima, F.-S.; Messagie, M.; Matheys, J.; Wynen, V.; Sergeant, N.; Van Mierlo, J.; De Vos, M.; De Caevel, B. Comparative LCA of Electric, Hybrid, LPG and Gasoline Cars in Belgian Context. *World Electr. Veh. J.* **2009**, *3*, 469–476. [CrossRef]
49. Merkisz, J.; Gallas, D.; Siedlecki, M.; Szymlet, N.; Sokolnicka, B. Exhaust Emissions of an LPG Powered Vehicle in Real Operating Conditions. *E3S Web Conf.* **2019**, *100*, 53. [CrossRef]
50. Mądziel, M. Liquified Petroleum Gas-Fuelled Vehicle CO_2 Emission Modelling Based on Portable Emission Measurement System, On-Board Diagnostics Data, and Gradient-Boosting Machine Learning. *Energies* **2023**, *16*, 2754. [CrossRef]

Disclaimer/Publisher's Note: The statements, opinions and data contained in all publications are solely those of the individual author(s) and contributor(s) and not of MDPI and/or the editor(s). MDPI and/or the editor(s) disclaim responsibility for any injury to people or property resulting from any ideas, methods, instructions or products referred to in the content.